THE JOURNAL OF BIOLOGICAL CHEMISTRY
Vol. 278, No. 50, Issue of December 12, pp. 50607–50614, 2003
Printed in U.S.A.

Tetrahydrobiopterin, a Critical Factor in the Production and Role of Nitric Oxide in Mast Cells*[S]

Received for publication, July 18, 2003, and in revised form, September 22, 2003
Published, JBC Papers in Press, September 26, 2003, DOI 10.1074/jbc.M307777200

Mark Gilchrist‡§, Christian Hesslinger¶, and A. Dean Befus‡‖

From the ‡Glaxo-Heritage Asthma Research Laboratory, Pulmonary Research Group, Department of Medicine, University of Alberta, Edmonton, Alberta T6G 2S2, Canada and ¶Pharmazentrum Frankfurt, J. W. Goethe-University, Frankfurt 60590, Germany

Mast cells (MC) are biologically potent, ubiquitously distributed immune cells with fundamental roles in host integrity and disease. MC diversity and function is regulated by exogenous nitric oxide; however, the production and function of endogenously produced NO in MC is enigmatic. We used rat peritoneal MC (PMC) as an *in vivo* model to examine intracellular NO production. Live cell confocal analysis of PMC using the NO-sensitive probe diaminofluorescein showed distinct patterns of intracellular NO formation with either antigen (Ag)/IgE (short term) or interferon-γ (IFN-γ) (long term). Ag/IgE-induced NO production is preceded by increased intracellular Ca^{2+}, implying constitutive nitric-oxide synthase (NOS) activity. NO formation inhibits MC degranulation. NOS has obligate requirements for tetrahydrobiopterin (BH_4), a product of GTP-cyclohydrolase I (CHI), IFN-γ-stimulated PMC increased CHI mRNA, protein, and enzymatic activity, while decreasing CHI feedback regulatory protein mRNA, causing sustained NO production. Treatment with the CHI inhibitor, 2,4-diamino-6-hydroxypyrimidine, inhibited NO in both IFN-γ and Ag/IgE systems, increasing MC degranulation. Reconstitution with the exogenous BH_4 substrate, sepiapterin, restored NO formation and inhibited exocytosis. Thus, Ag/IgE and IFN-γ induced intracellular NO plays a key role in MC mediator release, and alterations in NOS activity via BH_4 availability may be critical to the heterogeneous responsiveness of MC.

Mast cells are immune effector cells located at strategic tissue sites, juxtaposed to vessels, epithelium, and nerves. These phenotypic and functionally heterogeneous cells release granule-associated mediators (*e.g.* histamine) and various newly formed molecules (*e.g.* phospholipid metabolites and cytokines) that play roles in innate and adaptive immune responses (1). Classically, MC[1] can be activated via cross-linking of Fcε-bound IgE molecules by specific antigen (Ag), and inhibition of MC activation is a key component in controlling allergic diseases such as asthma (2). The T_H1 cytokine interferon-γ (IFN-γ) inhibits MC function, and dysregulation of IFN-γ contributes to atopy and asthma (2). IFN-γ modulation of cell phenotype is complex and involves regulation of gene expression (3) including the enzyme GTP-cyclohydrolase I (CHI), which produces tetrahydrobiopterin (BH_4) (4).

BH_4 is a critical factor in the production of the neurotransmitters serotonin, catecholamines, and other cellular activities including proliferation, cell cycle regulation, and differentiation (4). The majority of cellular BH_4 is synthesized *de novo* from GTP with CHI being rate-limiting (4). CHI activity is regulated at multiple levels, including transcription and phosphorylation, and can be inhibited by the CHI feedback regulatory protein (GFRP) (5, 6). BH_4 is also an essential co-factor in NO formation from nitric-oxide synthase (NOS), and increases in NOS transcription and activity need to be accompanied by a concurrent increase in BH_4 to sustain NO production (7).

NO is a reactive radical with pleotrophic effects with both physiological and pathological functions (8). NO is formed from L-arginine by the NOS family of isozymes that are subdivided on the basis of their Ca^{2+} dependence and transcriptional inducibility. Ca^{2+}-dependent members include endothelial (eNOS) and neuronal NOS (nNOS), characterized by constitutive expression and low NO production. Inducible NOS (iNOS) is up-regulated by a variety of inflammatory mediators and functions independently of cellular Ca^{2+} levels and releases large amounts of NO (8).

MC functions including degranulation and adhesion can be regulated by exogenous NO (9). We have recently shown that rat peritoneal MC (PMC) also constitutively express eNOS and can up-regulate iNOS and produce NO (10). More recent *in vivo* studies have implicated MC as a significant source of NO in vascular tissues, likely through nNOS (11). MC produce low amounts of NO, implying a paracrine, intracellular function. However, the roles for MC-derived NO remain poorly defined. Furthermore, our previous study showed that diverse stimuli induced differing levels of NO release from MC, despite similar induction of NOS (10). Clearly, other regulatory events are responsible for differences in the time course, quantities, and outcomes of MC-derived NO (12). Because no data are available on the role that BH_4 plays in NO production by MC, we hypothesized that post-transcriptional regulation of NOS activity by BH_4 is a critical determinant in NO production by MC.

* This work was supported by a grant from the Canadian Institutes for Health Research. The costs of publication of this article were defrayed in part by the payment of page charges. This article must therefore be hereby marked "*advertisement*" in accordance with 18 U.S.C. Section 1734 solely to indicate this fact.

[S] The on-line version of this article (available at http://www.jbc.org) contains a supplemental video.

§ Supported by a studentship from the Alberta Heritage Foundation for Medical Research. To whom correspondence should be addressed: Dept. of Medicine, Rm. 550 HMRC, University of Alberta, Edmonton, AB T6G 2S2, Canada. Tel.: 780-492-1909; Fax: 780-492-5329; E-mail: mark.gilchrist@ualberta.ca.

‖ AstraZeneca Canada Inc. Chair in Asthma Research.

[1] The abbreviations used are: MC, mast cell(s); Ag, antigen; IFN-γ, interferon-γ; CHI, cyclohydrolase I; BH_4, tetrahydrobiopterin; GFRP, CHI feedback regulatory protein; NOS, nitric-oxide synthase; eNOS, endothelial NOS; nNOS, neuronal NOS; iNOS, inducible NOS; PMC, peritoneal MC; cNOS, constitutive NOS; DAF, diaminofluorescein; L-NAME, N^G-nitro-L-arginine methyl ester; DAHP, 2,4-diamino-6-hydroxypyrimidine; DAF-FM, 4,5-diaminofluorescein diacetate; WE, worm equivalents; RT, reverse transcription; HPLC, high pressure liquid chromatography; β-hex, β-hexosaminidase.

The purpose of this study was 2-fold. First, to characterize both short term (<5 min) Ca^{2+}-dependent constitutive NOS (cNOS) activity and sustained NO formation (>18 h) in MC using the fluorescent NO-sensitive probe diaminofluorescein (DAF). Second, to investigate the effects of CHI activity and BH_4 levels in both short term (<5 min) and sustained (>18 h) NO production on MC reactivity. We demonstrate for the first time that a proportion of rat PMC dynamically activate intracellular Ca^{2+}-dependent NOS activity (<5 min) after Ag stimulation, which inhibits degranulation. Furthermore, IFN-γ treatment enhances long term (>18 h) intracellular NO production, which also inhibits MC degranulation. MC constitutively express CHI mRNA and protein, and upon stimulation with IFN-γ, PMC up-regulate CHI mRNA and protein with a concordant increase in CHI activity. IFN-γ also decreases GFRP mRNA levels. The final outcome of these events is an increased level of NO production after IFN-γ treatment. Thus, modulation of MC BH_4 levels controls NO formation and influences MC degranulation.

EXPERIMENTAL PROCEDURES

Animals—Adult male Sprague-Dawley (Crl:CD (SD) BR) rats were obtained from Charles River Canada Inc. (Quebec, Canada). For experiments requiring antigen stimulation, the rats were sensitized with L_3 larvae of *Nippostrongylus brasiliensis* 5–6 weeks before MC isolation (10). The experimental procedures were approved by the University Animal Care Committee and were in accordance with the guidelines of the Canadian Council on Animal Care.

Chemicals—The NOS inhibitor N^G-nitro-L-arginine methyl ester (L-NAME), NO donor *S*-nitrosoglutathione, and CHI inhibitor 2,4-diamino-6-hydroxypyrimidine (DAHP) were obtained from Calbiochem (San Diego, CA). The sepiapterin reductase inhibitor *N*-acetyl serotonin was obtained from Sigma, the pterin donor L-sepiapterin was obtained from Cayman Chemical (Ann Arbor, MI), and the NO probe 4,5-diaminofluorescein diacetate (DAF-FM) and Ca^{2+}-sensitive dye FURA-2 were obtained from Molecular Probes (Eugene, OR).

Antigen—Ag used to activate *in vivo* sensitized PMC was a collection of soluble excretory and secretory products of the nematode *N. brasiliensis*, prepared as previously described (13). The antigen concentration was described as worm equivalents (WE)/ml.

MC Isolation and Stimulation—PMC were obtained by peritoneal lavage followed by centrifugation through gradient Percoll as previously described (10). PMC purity was >98% as determined by staining with toluidine blue. Cell viability was >99%. For most experiments PMC from unsensitized rats were treated with medium containing IFN-γ (200 units/ml) (Invitrogen). For studies of MC secretion, PMC from *N. brasiliensis* sensitized rats were treated with Ag (5 WE/ml).

Live Cell Fluorescence Determination of Intracellular NO and Ca^{2+} Production—NO production by PMC was assayed using DAF-FM, a cell-permeable NO-sensitive fluorescent dye (14). Coverslip-bottomed Petri dishes (Falcon) were coated with rat plasma fibronectin (10 μg/ml) (Sigma) in phosphate-buffered saline, pH 7.2, for 1 h at 37 °C. PMC were loaded with 10 μM of DAF-FM. For Ca^{2+} experiments, PMC were loaded with FURA-2 (5 μM) and then incubated for 1 h at 37 °C in the dark. The cells were resuspended in RPMI 1640 without phenol red and placed in dishes and then incubated for 1 h at 37 °C before use.

The cell images were obtained using a Zeiss confocal laser scanning microscope (LSM510) using a 488-nm (excitation) and 505–530-nm (emission) filter set for DAF and a 340-nm (excitation) and 530-nm (emission) filter set for FURA-2, with a 40 × 1.3 oil Plan-Neofluar objective that was maintained at a constant 37 °C with a heating ring. Ag (5 WE/ml) was added to the cells, and DAF/FURA-2 fluorescence intensity was determined in real time, with 1-s exposures obtained every 5 s to avoid photobleaching. Because DAF fluorescence is almost linear with NO concentration, quantitative analysis of each cell (8–15 cells/experiment) was obtained by averaging the peak relative fluorescent intensity (optical density arbitrary units) (15). The percentage of change in fluorescence from base line (ΔF) was calculated by the equation $\Delta F = (F_b - F/F_b) \times 100$, where F_b is the basal fluorescence obtained from the frame before the addition of stimulus, and F is the fluorescence obtained after activation. The cells were defined as degranulating when they had ruffled membranes and had visibly extruded granules as previously described (16). Frame number and time reference were calculated using frame-by-frame analysis with MetaFluor imaging software (Universal Imaging Co., Downingtown, PA). In some experiments the NOS inhibitor L-NAME or the NO donor *S*-nitrosoglutathione was added 30 min before loading with DAF as negative and positive controls, respectively.

Reverse Transcription-PCR—Total RNA was isolated from PMC and pretreated with heparinase I (Sigma) as previously described (17). RT-PCR was performed on a PTC-100 Thermal Cycler (MJ Research, Boston, MA). The primers were designed to be intron-spanning based on published sequence data: CHI, sense, 5′-GATACCAGGAGACCATCTCA-3′, and antisense, 5′-TAGCATGGTGCTAG TGACAG-3′ (PCR product, 370 bp); and GFRP, sense, 5′-CCACTCACCATGCCCTACCT-3′, and antisense, 5′-GCAGCAAGGTTCCTGAGGCT-3′ (PCR product, 369 bp). The conditions for PCR amplification were as follows: denaturing at 95 °C for 45 s, annealing for 45 s, and extension at 72 °C for 1 min. The optimized annealing temperature was 48 °C for CHI and 50 °C for GFRP. The products were run on a 1.2% agarose gel and stained with ethidium bromide (Sigma).

Cloning and Sequencing of cDNA Bands—The amplified PCR products were subcloned into pCR2.1™ plasmid vector using the T/A cloning kit (Invitrogen). Plasmid DNA was isolated with the GenElute™ Plasmid isolation kit (Sigma). Double-stranded DNA sequencing was performed using M13 forward and reverse primers. Sequencing was conducted using an ABI 373A automated sequencer (Applied Biosystems, Foster City, CA) by a dideoxy chain termination method.

Semi-quantitative RT-PCR Using an External Standard—The linearized plasmid DNA containing the cloned inserts was used as a homologous amplification standard for semi-quantitative RT-PCR. Absorbance measurements at 260 nm were used to calculate the number of copies/μl. Known dilutions of the standard were amplified in concert with the unknown samples and separated by agarose electrophoresis. Band densitometry (SigmaGel, SPSS Science, Chicago, IL) was used to compare the intensities of the standards to the unknowns to obtain the relative number of copies/μl.

Western Blot Analysis—PMC were incubated in 24-well plates at 1×10^6 cells/well for 0–18 h in various experimental conditions. The cells were dissociated in RIPA buffer (phosphate-buffered saline, 1% Nonidet P-40). The total protein content was determined by the Bradford technique (Bio-Rad). Fifteen μg of protein from each sample was mixed with Laemmli buffer containing SDS and β-mercaptoethanol. The samples were separated on a 12% SDS-PAGE gel and transferred onto a polyvinylidene difluoride membrane (Bio-Rad). CHI was identified with rat monoclonal anti-CHI (6H11) (I. Ziegler, Munchen, Germany) (5) diluted 1/500 (1 μg/ml) and 1/5000 in horseradish peroxidase-conjugated goat anti-rat IgG (Serotec, Raleigh, NC). Labeling was detected by chemiluminescence with SuperSignal substrate solution (Pierce). The resulting bands were scanned and quantified in a gel scanner (ImageMaster DTS; Amersham Biosciences).

Immunofluorescence Detection of CHI—Localization of CHI in PMC was performed on PMC fixed in 4% paraformaldehyde for 20 min and then permeablized with 0.1% Triton X-100 in phosphate-buffered saline. The slides were blocked for 30 min with 10% fetal bovine serum and 3% bovine serum albumin in phosphate-buffered saline and then incubated overnight at 4 °C with 1 μg/ml of rat monoclonal CHI antibody (6H11). Specific antibody binding was detected with rhodamine red-labeled goat anti-rat antibody (Molecular Probes, Eugene, OR). Negative controls labeled with isotype (rat IgG1) antibody were run concurrently.

Enzyme Assay for CHI Activity—The activity of CHI was determined on homogenized cell extracts as previously described (5). Briefly, the reaction product was oxidized to neopterin triphosphate by acidic iodine solution. After reduction of excess iodine by ascorbic acid, the sample was immediately separated by ion pair reverse phase HPLC. Neopterin was then determined by reverse phase HPLC.

Measurement of NO_2^- Production—NO_2^- in culture (phenol red-free) supernatants was measured by the Griess reaction (10).

β-Hexosaminidase Assay—β-Hexosaminidase (β-hex) release was investigated as a functional measure of the BH_4/NO effects on granule mediator secretion as has been previously described (18).

Statistical Analysis—All of the experiments were performed at least three times. The data were analyzed using analysis of variance followed by the Bonferroni test for comparisons. p values < 0.01 were considered significant.

On-line Supplemental Material—Real time images of degranulation and NO production in Ag/IgE-stimulated MC are shown in the on-line supplemental video. The video image was obtained over a 4-min period, with 1-s exposures every 5 s. The video was compressed 10 times using Adobe Premiere (Adobe Systems Canada, Ottawa, Canada). The images were captured using a 40× objective on a Leica confocal laser scanning microscope. The video shows a flux of green DAF fluorescence in a

proportion of MC, which is correlated with inhibition of degranulation. MC that are negative for DAF degranulate quickly.

RESULTS

Sustained (>18 h) Intracellular Production of NO in IFN-γ-treated PMC—To confirm that IFN-γ treated PMC produced NO, we utilized the NO-specific fluorescent molecule DAF. Confocal microscopic analysis showed that IFN-γ caused an increase in intracellular DAF fluorescence after 18 h of treatment compared with controls. The DAF fluorescence localized to cytoplasmic and occasionally to perinuclear sites (Fig. 1*A*).

Real Time Confocal Analysis of IgE-mediated Degranulation and NO Production—Next we wanted to assess constitutive NOS activity because there is evidence that MC possess cNOS activity (19). To study this short term (<5 min) NOS activity, its modulation, and association with degranulation, we developed a real time assay to detect DAF fluorescence and analyze dynamic changes in NO production by individual cells. PMC were isolated and loaded with DAF (10 μM). A large proportion of unstimulated PMC showed weak DAF fluorescence, with an occasional cell (<2%) having stronger cytoplasmic fluorescence. PMC showed no visible signs of degranulation, because their membranes were intact and showed no signs of granule release as noted in other MC live cell studies (16).

Stimulation with Ag (5 WE/ml) caused an increase in the number of degranulating cells. Degranulating PMC did not shown any increases in DAF fluorescence (Fig 1*B* and the supplemental video). Interestingly a proportion (33.1 ± 2.2%, mean ± S.E. of 116 total cells in eight different experiments) of PMC showed an immediate (<2 min) increase in NO production (DAF fluorescence) and no visible signs of degranulation. DAF fluorescence accumulated in the cytoplasm of these cells, and a population of strong NO producing cells showed intense nuclear positivity (Fig. 1*B* and the supplemental video). Although the strong DAF fluorescence cells showed no sign of degranulation after 60 min of observation, some of the less positive cells eventually did show degranulation. Regression analysis comparing these weaker DAF fluorescent PMC to time of degranulation showed a highly significant correlation ($R^2 = 0.7056$, $p < 0.001$) (Fig. 1*C*). Equal loading of PMC with DAF was confirmed by adding the NO donor *S*-nitrosoglutathione (100 μM); after 20 min almost all PMC showed strong cytoplasmic staining with DAF (data not shown). Interestingly, no nuclear localization of DAF fluorescence was seen after adding this exogenous NO source. Specificity of the effect was determined by pretreating PMC with the NOS inhibitor L-NAME (100 μM); these cells showed no flux of DAF fluorescence (data not shown). These results support the hypothesis that PMC possess cNOS activity that can be stimulated in the short term (<5 min) in a proportion of cells by IgE cross-linking. Our data also suggest that immediate NO production by PMC causes inhibition of mediator release.

Ca^{2+} Flux and NO Production in PMC—The results above may involve constitutive NOS (eNOS or nNOS) activity in PMC (10). Because both eNOS and nNOS are Ca^{2+}-dependent, we wished to determine whether increases in intracellular Ca^{2+} precede the flux of NO seen in Ag/IgE-treated PMC. PMC were isolated and loaded with both DAF (10 μM) and the Ca^{2+}-sensitive dye FURA-2 (5 μM). As has been previously shown, upon stimulation with Ag (5 WE/ml), all PMC showed an increase in FURA-2 fluorescence beginning within 30 s (Fig. 1*B*) (20). DAF fluorescence in strong NO producing cells was delayed by almost 20 s on average compared with FURA-2 (Fig. 1*D*). However, DAF fluorescence in degranulating MC showed little change (Fig. 1*E*) Interestingly, although PMC were heterogeneous in their DAF positivity, all cells were homogenous in their Ca^{2+} flux (Fig. 1, *D* and *E*). This indicates that Ca^{2+} flux precedes short term NO production in nondegranulating, Ag-treated PMC.

GTP-CHI/GFRP mRNA Expression in PMC—We recently showed that rat PMC treated with IFN-γ could be stimulated to express iNOS mRNA (10); however, no data exist concerning the expression of CHI or GFRP in *in vivo* derived MC. mRNA production was thus determined using RT-PCR with gene-specific primers. PMC constitutively express significant CHI and GFRP mRNA. (Fig. 2). All of the PCRs were negative when the RT step was eliminated, indicating that there was no contamination from genomic DNA (data not shown). Cloned PCR amplicons were sequenced and showed >98% identity with published sequences by BLAST (NCBI) analysis.

Differential Regulation of GTP-CHI and GFRP mRNA—Because stimuli that increase NOS expression often induce a concordant increase in *de novo* BH_4 production (7), we looked at CHI and GFRP mRNA regulation by IFN-γ. Total RNA was extracted from unstimulated PMC (>98% pure) and from PMC treated *in vitro* with IFN-γ (200 units/ml). CHI and GFRP mRNA production was assessed by semiquantitative RT-PCR *versus* a standard curve constructed with known copy numbers of cloned inserts amplified under identical PCR conditions. Within 2 h following treatment with IFN-γ, the CHI signal in PMC increased ~3-fold. Levels of CHI mRNA reached maximal expression at 6 h and continued to increase to 18 h (Fig. 2*A*). No change in CHI mRNA was noted in unstimulated PMC at similar time points (data not shown). GFRP mRNA expression from IFN-γ-treated PMC was significantly down-regulated beginning at 2 h and continued until at least 18 h of treatment (Fig. 2*B*). The results are from PMC RNA obtained from three independent batches of cells.

CHI Protein Expression—To further evaluate whether the actions of IFN-γ on GTP-CHI mRNA levels were extended to protein expression, Western blot analysis was employed. Unstimulated PMC constitutively produced a band of 30 kDa detected by the antibody 6H11 (Fig. 3*A*). Exposure of PMC to IFN-γ produced a significant increase in CHI protein expression, with maximal stimulation between 6 and 18 h. Again unstimulated PMC cultured during the same time showed no increase in CHI protein expression. Furthermore, PMC stimulated with Ag/IgE also showed no detectable change in protein expression (data not shown).

Immunofluorescence Localization of CHI in Rat MC—Because the intracellular localization of CHI is poorly understood, we used confocal laser scanning microscopy to assess the cellular expression pattern of CHI protein in PMC. Unstimulated PMC from naïve rats showed a clear plasma membrane pattern with some nuclear immunofluorescence in occasional cells. Membrane staining was confirmed by imaging en face 0.5-μm sections through each cell. This stacked series of multiple images was deconvoluted and three-dimensionally reconstructed using Zeiss LSM 510 software. PMC stimulated with IFN-γ, on the other hand, showed a pronounced increase in cytosolic immunofluorescence while maintaining membrane and some nuclear labeling (Fig. 3*B*).

CHI Enzymatic Activity—To determine the functional consequences of IFN-γ treatment, we determined CHI enzymatic activity, employing a HPLC-based assay as previously described (5). Untreated PMC were compared with cells treated with IFN-γ or Ag/IgE. In unstimulated cells, CHI activity was low (<5.0 nmol/mg/min) as previously described (5) but was markedly elevated upon treatment with IFN-γ with a significant increase observed at 6 h that continued to at least 18 h (Fig. 4). As expected from Western blot data, no increase in CHI activity was seen after Ag/IgE treatments (data not shown).

Control of PMC NO (>18 h) Production by BH_4—Previously,

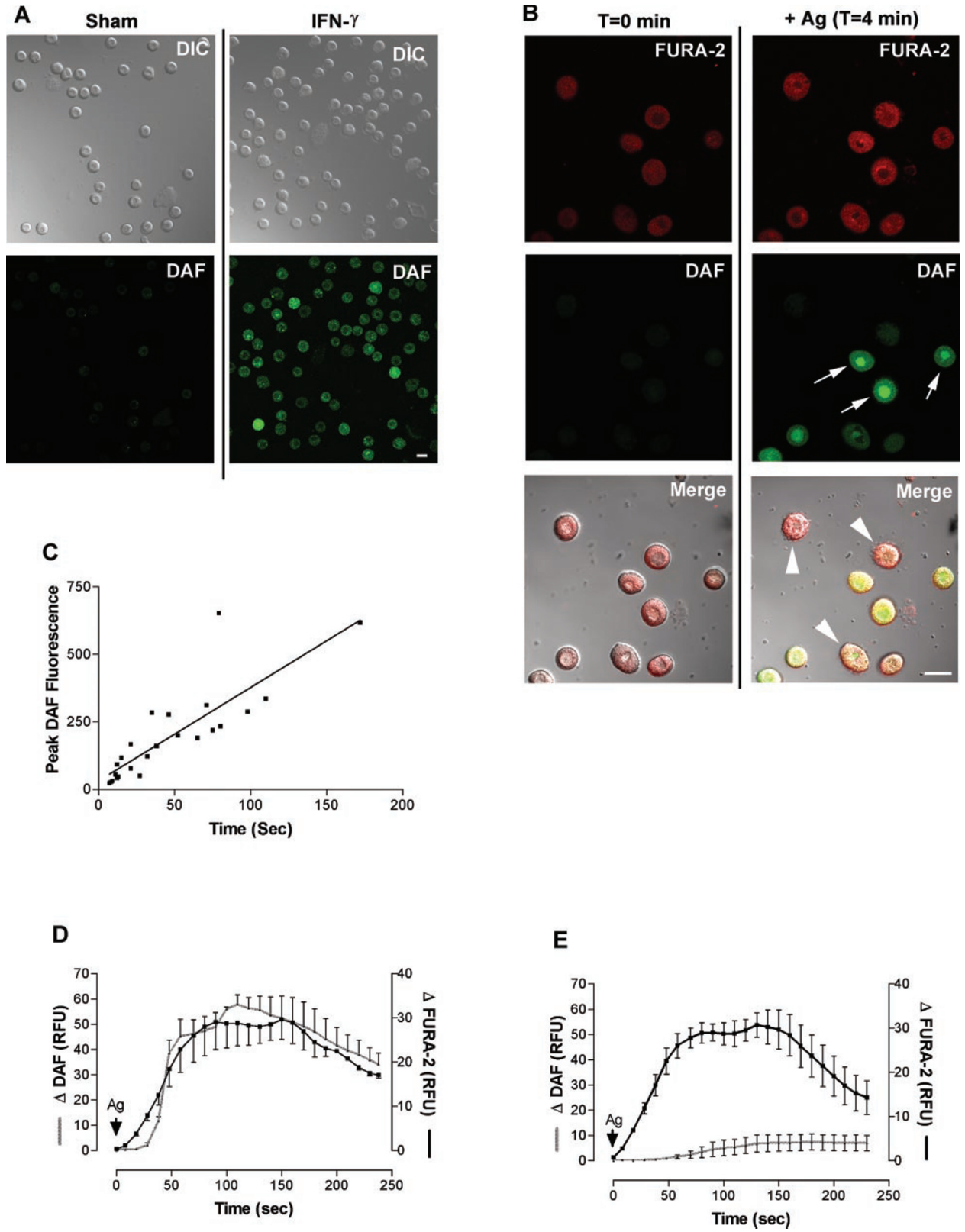

FIG. 1. *A*, fluorescence detection of intracellular NO production in PMC. The cells were incubated with IFN-γ (200 units/ml) for 18 h and then stained with DAF for 20 min. DAF fluorescence (*green*) was visualized by confocal analysis. Untreated PMC are used as the control. Differential interference contrast (*DIC*) shows cellular morphology. Original magnification, ×400; *bar*, 10 μm. The values are representative of four independent experiments. *B*, real time confocal analysis of Ca^{2+} accumulation and NO production in Ag-stimulated PMC. PMC from sensitized rats were loaded with both DAF (10 μM) and FURA-2 (5 μM) for 1 h. The cells were stimulated with Ag, and images were simultaneously obtained every 5 s from both DAF and FURA-2 channels. The panels show representative DAF (*green*), FURA-2 (*red*), and combined images (*yellow*) obtained before the addition of Ag ($t = 0$) and at a time point when no further changes in PMC morphology were observed ($t = 4$ min). *White arrowheads* indicate degranulating cells, and *white arrows* indicate nuclear accumulation of DAF in PMC nucleus. Original magnification, ×600; *bar*, 10 μm. The results are representative of three independent experiments. The complete video is available as supplementary information. *C*, correlation between NO production (peak DAF fluorescence; arbitrary units) and time to degranulation (seconds) from Ag-stimulated MC that produce NO but later show signs of degranulation. The data shown are from 30 individual MC from five independent experiments. Linear regression analysis was

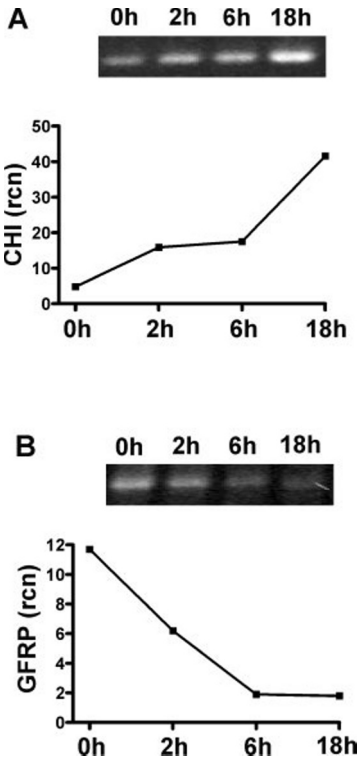

FIG. 2. **Semiquantitative RT-PCR analysis of CHI (*A*) and GFRP (*B*) mRNA expression in PMC treated with IFN-γ (200 units/ml).** RNA from IFN-γ-treated PMC were isolated at indicated time points and analyzed by RT-PCR *versus* known concentrations of homologous cloned standard. Band densitometries from the standards were used to determine the relative copy number (*rcn*) in each of the IFN-γ-treated samples. Graphic representation of the time course with responses plotted as relative copy number. The data are from one representative experiment. Similar results were seen with three separate batches of PMC ($n = 3$).

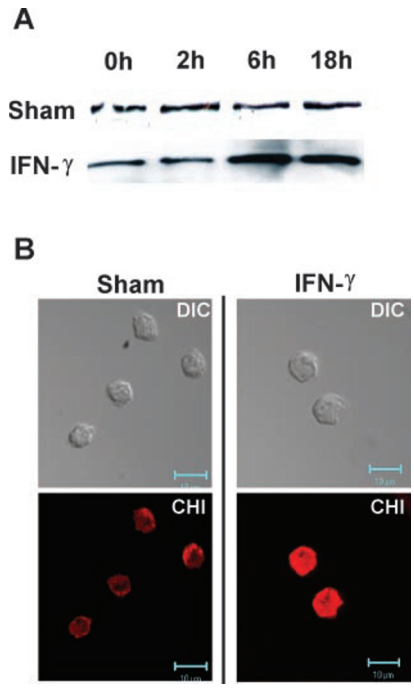

FIG. 3. **CHI protein analysis.** *A*, Western blot analysis using anti-CHI antibody (6H11) with 15 μg of total cell lysate obtained from PMC treated with IFN-γ (200 units/ml) for the indicated times. As a control, lysates from untreated PMC incubated for identical times were also analyzed. The results are representative of three separate experiments. *B*, confocal analysis of CHI localization in sham control and IFN-γ-treated PMC. Differential interference contrast (*DIC*) shows cell in the field. CHI immunofluorescence is shown in *red*. CHI is detected in the plasma membrane via imaging 0.5-μm optical en face sections throughout the cell. Original magnification, ×800; *bar*, 10 μm.

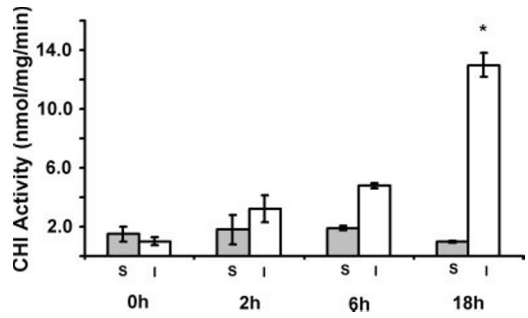

FIG. 4. **Time course analysis of CHI enzymatic activity in PMC cultured with (*I*) or without (*S*) IFN-γ (200 units/ml).** PMC were incubated for the indicated times, and cell pellets were obtained. BH_4 production was then determined by reverse phase HPLC. The data are shown as nmol/mg/min (means ± S.E. of three separate experiments).

PMC have been shown to produce NO (10). Unstimulated PMC spontaneously released low levels of NO_2^- (0.27 ± 0.03 μM). Activation with IFN-γ caused PMC to produce significantly greater ($p < 0.01$) amounts of NO_2^- (3.6 ± 0.2 μM). (Fig. 5). To further define the role of CHI and BH_4 in MC NO production, we employed the pharmacological inhibitor of CHI (DAHP) (4). The addition of DAHP along with IFN-γ for 24 h inhibited NO production in a dose-dependent manner (Fig. 5). To further confirm that PMC cellular BH_4 levels were limiting in NO production, the cells were treated with an exogenous substrate for BH_4 production, sepiapterin. Sepiapterin treatment slightly (but not significantly) potentiated NO production in untreated cells and increased nitrite accumulation upon IFN-γ stimulation (4.6 ± 0.3 μM) (Fig. 5). Significant inhibition ($p < 0.01$) was attained with DAHP concentrations as low as 100 μM, with nitrite levels at or below sham values with concentrations of 500 μM. Because DAHP at high concentrations (500 μM) completely inhibit nitrite formation, there appears to be little contribution via the salvage pathway under these conditions. These results were confirmed using the sepiapterin reductase inhibitor *N*-acetyl serotonin (data not shown). However, coadministration of DAHP (500 μM) with 200 μM sepiapterin significantly ($p < 0.01$) reconstituted nitrite production (3.2 ± 0.1 μM) (Fig. 5).

Effects of BH_4 Modulation (>18 h) on MC Degranulation—Given the above results showing that BH_4 levels are important in regulating MC NO production, we investigated the effects of IFN-γ and modulation of BH_4 on MC degranulation by measuring β-hex release. PMC were treated for 18 h with IFN-γ (200 units/ml), DAHP (500 μM), or sepiapterin (200 μM) and then

used, and the correlation is highly significant ($p < 0.001$). *D*, temporal relationship between Ca^{2+} and NO in PMC after Ag stimulation. Changes in the average pixel intensity (Δ) for both DAF (NO; *gray line*) and FURA-2 (Ca^{2+}; *black line*) in nondegranulating PMC were plotted *versus* time (seconds) after the addition of Ag. Each line represents the average change in fluorescence (mean ± S.E.) for 3–7 cells from one field of a representative experiment. *E*, changes in the average pixel intensity (Δ) for both DAF (NO; *gray line*) and FURA-2 (Ca^{2+}; *black line*) in degranulating PMC were plotted *versus* time (seconds) after addition of Ag. Each line represents the average change in fluorescence (mean ± S.E.) for 3–7 cells from one field of a representative experiment. The results are representative of three separate experiments. The data are expressed as relative fluorescence units (*RFU*).

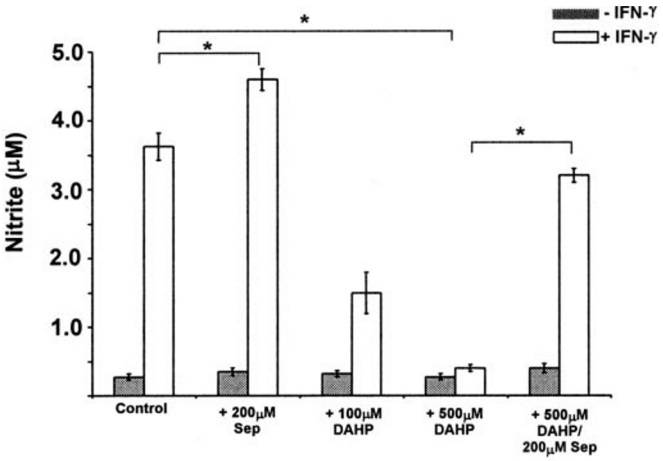

FIG. 5. **The effect of BH_4 modulation on PMC NO production (nitrite) measured by the Griess assay.** PMC treated with the alternate pterin substrate sepiapterin (*Sep*) (200 μM) were used to determine whether increased BH_4 availability effects NO production. The cells treated with IFN-γ and the CHI inhibitor DAHP (100 and 500 μM) were used to determine the effect of decreased BH_4 levels on NO production. The addition of sepiapterin (200 μM) was used to reconstitute BH_4 levels in DAHP-treated PMC. The cells from unsensitized rats were used as the sham control. The data are shown as the means ± S.E. of three experiments, 2×10^5 cells/sample were analyzed. The *asterisk* indicates $p < 0.01$ by comparison with untreated cells.

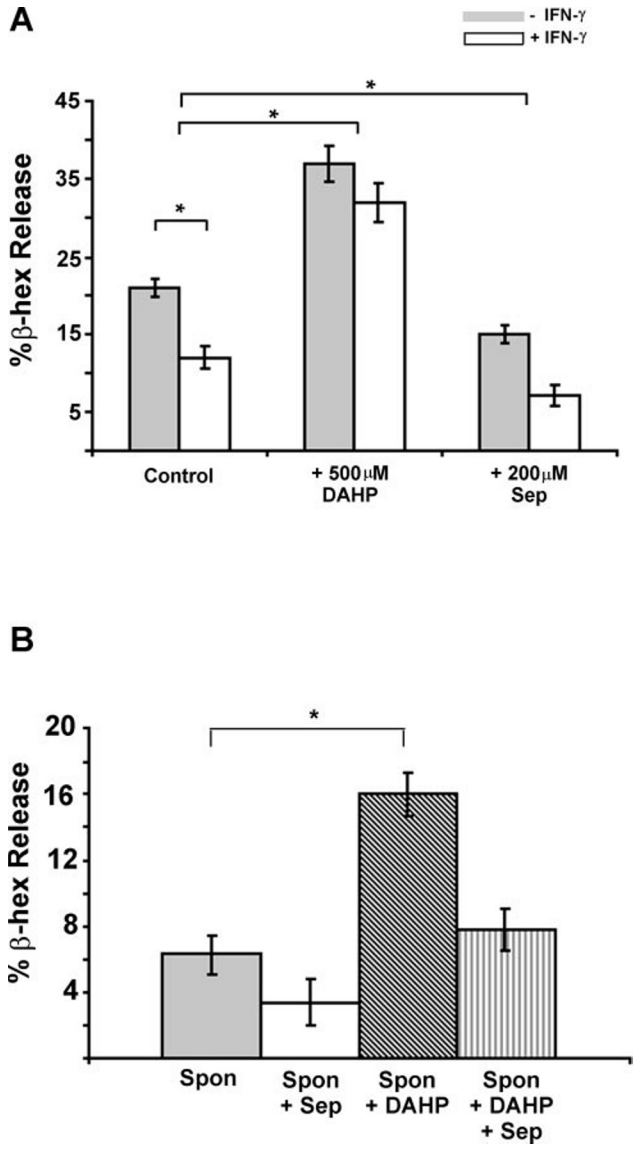

FIG. 6. *A*, effects of BH_4 availability on β-hex release from PMC. PMC from sensitized rats were cultured for 18 h with (*open bars*) and without (*shaded bars*) IFN-γ (200 units/ml) and then stimulated with Ag for 20 min, and β-hex release was measured. PMC were also treated with or without IFN-γ in the presence of DAHP (500 μM) or sepiapterin (*Sep*) (200 μM) for 18 h and then stimulated with Ag for 20 min. *B*, effects of BH_4 modulation on spontaneous β-hex release (*Spon*). PMC were treated for 18 h in the presence of DAHP (500 μM), sepiapterin (200 μM), or both, and spontaneous release of β-hex was measured and compared with release from untreated PMC. The data are shown as mean ± S.E. of three experiments. The *asterisk* indicates $p < 0.01$.

stimulated with Ag (5 WE/ml) for 30 min. As Fig. 6*A* shows, Ag stimulation induced 21 ± 1.2% release, whereas IFN-γ treatment significantly ($p < 0.05$) inhibited Ag-induced release by over 40% (11 ± 1.5% release). Pretreatment of PMC with DAHP (500 mM) for 24 h resulted in a significant ($p < 0.05$) increase in Ag-induced β-hex release (from 21 ± 1.2% to 37 ± 2.3%) and abrogated the inhibitory effect of IFN-γ. Treatment with sepiapterin induced significant ($p < 0.05$) inhibition of β-hex release after Ag stimulation in IFN-γ and untreated PMC. Furthermore, modulation of BH_4 levels also influenced spontaneous β-hex release (Fig. 6*B*). PMC spontaneously release about 6% (6.3 ± 0.9%) β-hex. DAHP pretreatment significantly ($p < 0.01$) increased spontaneous β-hex release (16.1 ± 1.3%). Interestingly, sepiapterin also caused a modest but not significant inhibition of spontaneous release (Fig. 6*B*).

Effects of BH_4 Inhibition on Short Term (<5 min) NO Production/MC Degranulation—The results obtained above indicated that DAHP and sepiapterin modulate MC NO production long term (>18 h) and thus regulate degranulation. Because BH_4 is a critical co-factor for all NOS isoforms, we studied the effects of DAHP on Ca^{2+}-dependent NOS activity and degranulation. PMC from sensitized rats were isolated and loaded with DAF (10 μM); some cells were first pretreated with DAHP (500 μM) for 6 h before loading. PMC were then treated with Ag and analyzed by real time confocal microscopy as outlined above. DAHP-treated MC showed increased membrane changes, with some degranulating MC clearly evident (Fig. 7). Furthermore, DAHP-treated PMC showed no NO flux compared with untreated controls, and most cells degranulated in <3 min.

DISCUSSION

NO is a known modulator of both pro- and anti-inflammatory MC functions, although regulation of its endogenous production is unknown (9). These diverse effects imply a complex regulatory mechanism to control the timing, amounts, and location of NO production (8). Because BH_4 is a critical NOS co-factor, we investigated the expression and regulation of BH_4 production in MC and its role in regulating long (inducible) and short term (constitutive) NOS activity and the resulting effect on MC secretion.

Using the fluorescent NO marker, DAF, we identified both long (iNOS) and short term (cNOS) intracellular NO production in PMC. We have previously shown iNOS up-regulation in PMC following IFN-γ treatment (10). DAF staining in IFN-γ (long term) treated PMC showed a diffuse cytoplasmic pattern with possible Golgi staining in some cells. Earlier studies by ourselves and others have indicated that PMC may also have Ca^{2+}-dependent NOS activity by eNOS or nNOS (10, 11). A proportion of PMC treated with Ag/IgE showed immediate (short term) NO formation preceded by a flux in Ca^{2+} levels. Because both cNOS isoforms are Ca^{2+}-dependent for their activity, our results support a functional cNOS in MC.

IFN-γ is an important T_H1 cytokine and is a potent inhibitor of T_H2 type responses including those involving MC. Our data show a significant (8-fold) potentiation of CHI mRNA expres-

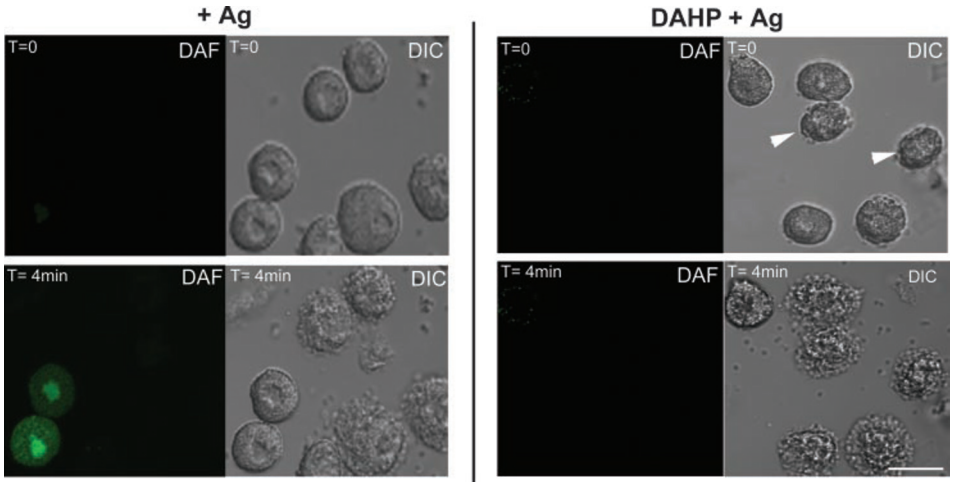

FIG. 7. **Real time confocal analysis of the effects of BH_4 inhibition on Ag-induced NO production and degranulation.** PMC from sensitized rats were treated with or without DAHP (500 μM), loaded with DAF (10 μM), and stimulated with Ag. Live images of Ag-stimulated PMC were obtained every 5 s. The panels show representative DAF fluorescence (*green*) and combined (*DAF + DIC*) images obtained before the addition of Ag ($t = 0$) and at a time point where no further changes in PMC morphology were observed ($t = 4$ min). The *white arrowheads* indicate degranulating cells. Original magnification, ×600; *bar*, 10 μm. The results are representative of eight separate experiments.

sion upon treatment with IFN-γ. Because CHI is a well known IFN-γ-inducible gene, these data are consistent with that shown for other cells types (21, 22). We also investigated the mRNA expression of a CHI regulatory protein, GFRP (23). IFN-γ significantly down-regulates GFRP mRNA production in PMC, which coincides with increased CHI production. By contrast, in C6 (glioblastoma) cells, IFN-γ or interleukin-1β caused an increase in CHI expression with no effect on GFRP, whereas in THP-1 (myelomonocytoma) cells, GFRP was unaltered by IFN-γ or interleukin-1β but instead was down-regulated by lipopolysaccharide (24, 25). IFN-γ thus has a unique regulatory effect on PMC that potentiates BH_4 production through increased CHI and inhibiting GFRP expression.

The Western blot data confirm that IFN-γ up-regulates CHI protein expression in a similar manner. We also showed that IFN-γ treatment increased CHI enzymatic activity and BH_4 accumulation in PMC as seen in other cell types (21). This increased expression is associated with altered localization of CHI in PMC. In untreated PMC there is a distinct membranous localization of CHI with occasional nuclear positivity but little cytoplasmic staining. Treatment with IFN-γ results in a pronounced increase in the cytoplasmic accumulation of CHI. Previous studies in neurons have shown both cytoplasmic and nuclear CHI staining (26). Our data are novel in that we show for the first time a membranous localization of CHI. A possible explanation for distinct localization patterns of CHI may be that BH_4 is highly labile *in vivo*, and CHI may need to be in close proximity to NOS to maintain adequate BH_4 levels and NO production (4). As such, our immunohistochemistry results (10) and that from others have shown a diffuse cytoplasmic pattern of iNOS expression in MC (27), a similar intracellular location to our DAF results with IFN-γ. Thus, co-localization of iNOS and CHI may contribute to increased NO production after IFN-γ treatment.

BH_4 is an important co-factor for all NOS isoforms. Using the CHI inhibitor DAHP and sepiapterin reductase inhibitor *N*-acetyl serotonin, we demonstrated that diminishing BH_4 leads to decreased NO. Decreased NO production through direct inhibition of NOS has been previously shown to potentiate MC degranulation (28). We found similar results, because inhibition of BH_4 production increased mediator release from PMC. Furthermore, the inhibitory effect of IFN-γ (18 h) treatment on PMC degranulation was removed by DAHP, implying that the IFN-γ effect was BH_4-dependent. Our results using DAHP and *N*-acetyl serotonin are similar to those seen with mouse macrophages, although higher concentrations of inhibitor were necessary to inhibit NO in those studies (29–31). Because both cell types constitutively express CHI, this disparity may point to differences in compartmentalization of CHI and NOS (30).

We previously showed that NO production in naïve PMC likely relies on cNOS activity (10). PMC treated with DAHP, sepiapterin, or both but without a known secretagogue showed modulation of degranulation. Therefore regulation of BH_4 levels is also important in cNOS activity in PMC. Our results using live cell analysis further support these findings because DAHP inhibited NO production and increased degranulation.

Levels of BH_4 are a determining factor in the reactive radicals derived from NOS because the NOS dimer may produce superoxide (O_2^-) or peroxynitrite ($ONOO^-$) rather than NO (32). Interestingly, O_2^- potentiates MC secretion, although the source of O_2^- is unknown (28). It is interesting to speculate that O_2^- arises in MC from NOS that is not saturated with BH_4. Indeed, previous studies using the NOS inhibitor L-NAME showed decreased NO and a resulting increase in O_2^- production and MC degranulation (28, 33). Interestingly, L-NAME also inhibits the reductase region of the NOS enzyme, causing the preferential formation of O_2^- (34). Thus, NOS may maintain a redox balance in MC by producing NO or ONOO to inhibit degranulation, and removal of BH_4 leads to O_2^- production and degranulation. This hypothesis requires further study.

Previous studies have shown that Ag/IgE activation of MC causes a transient hyperphosphorylation of CHI and increase in cellular BH_4 (5), and this was interpreted to be an activation step prior to degranulation, although the exact role for this increased BH_4 production was unknown. Our live cell results add a caveate to these results, because this increased BH_4 production appears to coincide with our noted NO production in MC after Ag/IgE activation. BH_4 levels may thus play a key role in controlling MC degranulation via NO, and cellular localization of BH_4 and its role in NO production require further investigation.

The nuclear localization of NO is to our knowledge the first identification of dynamic accumulation of NOS activity in the nucleus. Previous studies show eNOS protein in nuclear and perinuclear regions (35, 36). Furthermore, studies have shown both Ca^{2+} and calmodulin accumulation at nuclear sites in activated MC (20, 37). Because both Ca^{2+} and calmodulin are

critical in NOS activity, there may be a nuclear/NOS axis, although a role for NO in the nucleus is unknown (38).

Live cell imaging has allowed the investigation of MC functional heterogeneity and NO production at the single cell level. Furthermore, the differing localization of DAF positivity in IFN-γ- and Ag/IgE-treated MC implies involvement of distinct regulatory mechanisms. This pattern of DAF positivity was divergent from that seen when DAF-loaded MC were treated with an NO donor. Thus, interpretation of data in NO studies of MC function will have to carefully consider the source of NO because they may have potentially divergent outcomes and molecular mechanisms

In conclusion, we have characterized both short and long term intracellular NO production in MC and showed that increased intracellular NO production is associated with inhibition of Ag-induced degranulation. Furthermore, BH_4 levels are critical to sustaining NO production in MC and can regulate MC degranulation. Further study of NO regulatory pathways such as through BH_4 will help define novel molecular targets that modulate MC-related inflammatory and innate responses.

REFERENCES

1. Wedemeyer, J., Tsai, M., and Galli, S. J. (2000) *Curr. Opin. Immunol.* **12,** 624–631
2. Busse, W. W., and Rosenwasser, L. J. (2003) *J. Allergy Clin. Immunol.* **111,** S799–S804
3. Ramana, C. V., Gil, M. P., Schreiber, R. D., and Stark, G. R. (2002) *Trends Immunol.* **23,** 96–101
4. Thony, B., Auerbach, G., and Blau, N. (2000) *Biochem. J.* **347,** 1–16
5. Hesslinger, C., Kremmer, E., Hultner, L., Ueffing, M., and Ziegler, I. (1998) *J. Biol. Chem.* **273,** 21616–21622
6. Milstien, S., Jaffe, H., Kowlessur, D., and Bonner, T. I. (1996) *J. Biol. Chem.* **271,** 19743–19751
7. Togari, A., Arai, M., Mogi, M., Kondo, A., and Nagatsu, T. (1998) *FEBS Lett.* **428,** 212–216
8. Alderton, W. K., Cooper, C. E., and Knowles, R. G. (2001) *Biochem. J.* **357,** 593–615
9. Coleman, J. W. (2002) *Clin. Exp. Immunol.* **129,** 4–10
10. Gilchrist, M., Savoie, M., Nohara, O., Wills, F. L., Wallace, J. L., and Befus, A. D. (2002) *J. Leukocyte Biol.* **71,** 618–624
11. Kashiwagi, S., Kajimura, M., Yoshimura, Y., and Suematsu, M. (2002) *Circ. Res.* **91,** e55–e64
12. Grisham, M. B., Jourd'Heuil, D., and Wink, D. A. (1999) *Am. J. Physiol.* **276,** G315–G321
13. Lee, T. D., Shanahan, F., Miller, H. R., Bienenstock, J., and Befus, A. D. (1985) *Immunology* **55,** 721–728
14. Suzuki, N., Kojima, H., Urano, Y., Kikuchi, K., Hirata, Y., and Nagano, T. (2002) *J. Biol. Chem.* **277,** 47–49
15. Itoh, Y., Ma, F. H., Hoshi, H., Oka, M., Noda, K., Ukai, Y., Kojima, H., Nagano, T., and Toda, N. (2000) *Anal. Biochem.* **287,** 203–209
16. Williams, R. M., Shear, J. B., Zipfel, W. R., Maiti, S., and Webb, W. W. (1999) *Biophys. J.* **76,** 1835–1846
17. Gilchrist, M., MacDonald, A. J., Neverova, I., Ritchie, B., and Befus, A. D. (1997) *J. Immunol. Methods* **201,** 207–214
18. Kulka, M., Gilchrist, M., Duszyk, M., and Befus, A. D. (2002) *J. Leukocyte Biol.* **71,** 54–64
19. Hogaboam, C. M., Befus, A. D., and Wallace, J. L. (1993) *J. Immunol.* **151,** 3767–3774
20. Mori, S., Saino, T., and Satoh, Y. (2000) *Arch. Histol. Cytol.* **63,** 261–270
21. Schott, K., Gutlich, M., and Ziegler, I. (1993) *J. Cell. Physiol.* **156,** 12–16
22. Delgado-Esteban, M., Almeida, A., and Medina, J. M. (2002) *J. Neurochem.* **82,** 1148–1159
23. Kapatos, G., Hirayama, K., Shimoji, M., and Milstien, S. (1999) *J. Neurochem.* **72,** 669–675
24. Werner, E. R., Bahrami, S., Heller, R., and Werner-Felmayer, G. (2002) *J. Biol. Chem.* **277,** 10129–10133
25. Vann, L. R., Twitty, S., Spiegel, S., and Milstien, S. (2000) *J. Biol. Chem.* **275,** 13275–13281
26. Dassesse, D., Hemmens, B., Cuvelier, L., and Resibois, A. (1997) *Brain Res.* **777,** 187–201
27. Messina, A., Knight, K. R., Dowsing, B. J., Zhang, B., Phan, L. H., Hurley, J. V., Morrison, W. A., and Stewart, A. G. (2000) *Lab. Invest.* **80,** 423–431
28. Niu, X. F., Ibbotson, G., and Kubes, P. (1996) *Circ. Res.* **79,** 992–999
29. Werner-Felmayer, G., Werner, E. R., Fuchs, D., Hausen, A., Reibnegger, G., Schmidt, K., Weiss, G., and Wachter, H. (1993) *J. Biol. Chem.* **268,** 1842–1846
30. Sakai, N., Kaufman, S., and Milstein, S. (1993) *Mol. Pharmacol.* **43,** 6–10
31. Kasai, K., Hattori, Y., Banba, N., Hattori, S., Motohashi, S., Shimoda, S., Nakanishi, N., and Gross, S. S. (1997) *Am. J. Physiol.* **273,** H665–H672
32. Vasquez-Vivar, J., and Kalyanaraman, B. (2000) *FEBS Lett.* **481,** 305–306
33. Brooks, A. C., Whelan, C. J., and Purcell, W. M. (1999) *Br. J. Pharmacol.* **128,** 585–590
34. Wang, W., Wang, S., Yan, L., Madara, P., Del Pilar, C. A., Wesley, R. A., and Danner, R. L. (2000) *J. Biol. Chem.* **275,** 16899–16903
35. Giordano, A., Tonello, C., Bulbarelli, A., Cozzi, V., Cinti, S., Carruba, M. O., and Nisoli, E. (2002) *FEBS Lett.* **514,** 135–140
36. Govers, R., van der, S. P., van Donselaar, E., Slot, J. W., and Rabelink, T. J. (2002) *J. Histochem. Cytochem.* **50,** 779–788
37. Sullivan, R., Burnham, M., Torok, K., and Koffer, A. (2000) *Cell Calcium* **28,** 33–46
38. Kim, S. O., Merchant, K., Nudelman, R., Beyer, W. F., Jr., Keng, T., DeAngelo, J., Hausladen, A., and Stamler, J. S. (2002) *Cell* **109,** 383–396